

ARTICLE

<https://doi.org/10.1038/s42003-019-0746-2>

OPEN

The PHD finger of *Arabidopsis* SIZ1 recognizes trimethylated histone H3K4 mediating SIZ1 function and abiotic stress response

Kenji Miura ^{1,2,3*}, Na Renhu^{1,3} & Takuya Suzaki^{1,2}

Arabidopsis SIZ1 encodes a SUMO E3 ligase to regulate abiotic and biotic stress responses. Among SIZ1 or mammalian PIAS orthologs, plant SIZ1 proteins contain the plant homeodomain (PHD) finger, a C₄HC₃ zinc finger. Here, we investigated the importance of PHD of *Arabidopsis* SIZ1. The *Pro*_{SIZ1}::SIZ1(Δ PHD):GFP was unable to complement growth retardation, ABA hypersensitivity, and the cold-sensitive phenotype of the *siz1* mutant, but *Pro*_{SIZ1}::SIZ1:GFP could. Substitution of C162S in the PHD finger was unable to complement the *siz1* mutation. Tri-methylated histone H3K4 (H3K4me₃) was recognized by PHD, not by PHD (C162S). WRKY70 was up-regulated in the *siz1*-2 mutant and H3K4me₃ accumulated at high levels in the WRKY70 promoter. PHD interacts with ATX, which mediates methylation of histone, probably leading to suppression of ATX's function. These results suggest that the PHD finger of SIZ1 is important for recognition of the histone code and is required for SIZ1 function and transcriptional suppression.

¹Graduate School of Life and Environmental Sciences, University of Tsukuba, Tsukuba 305-8572, Japan. ²Tsukuba-Plant Innovation Research Center (T-PIRC), University of Tsukuba, Tsukuba 305-8572, Japan. ³These authors contributed equally: Kenji Miura, Na Renhu. *email: miura.kenji.ga@u.tsukuba.ac.jp

Sumoylation, the covalent attachment of small ubiquitin-like modifier (SUMO) to other proteins, is a post-translational modification that controls protein function, activity, localization, and turnover in eukaryotes^{1,2}. In plants, sumoylation is involved in the response to abiotic and biotic stresses, such as cold, salt, and drought stresses, and innate immunity^{3–8}. Furthermore, sumoylation regulates signaling pathways for plant hormones, including abscisic acid (ABA) and salicylic acid^{7,9–12}. Similar to ubiquitin, three enzymes, E1, E2, and E3, are required for the attachment of SUMO to other proteins². E1, the heterodimeric SUMO-activating enzyme, which is composed of the SAE1 and SAE2 subunits, binds to SUMO via a high-energy thioester linkage^{13,14}. Activated SUMO is transferred to E2, SUMO-conjugating enzyme 1 (SCE1) via transesterification, and then conjugated to substrate proteins, assisted by E3, SUMO ligase^{15,16}, via an isopeptide bond between the C-terminal glycine of SUMO and specific lysine(s) within the target. SUMO is often conjugated to lysine in the conserved ΨKXE/D (Ψ, a large hydrophobic amino acid; K, lysine; X, any amino acid; E, glutamate; and D, aspartate) motifs. At the molecular level, sumoylation alters the function of the targets, including changes in their intracellular localization, activity, and interaction with other proteins¹⁷. Previous proteomic studies have identified over 1000 SUMO1/2 targets in *Arabidopsis*^{18,19}. Most of these targets are nuclear-localized proteins and these proteins have functions related to DNA modification, chromatin assembly, transcription factors, coactivators/repressors, and abiotic and biotic stress responses¹⁹.

In *Arabidopsis*, four SUMO E3 ligases have been identified; SAP and MIZ1 domain-containing ligase1 (SIZ1)¹⁵, methyl methanesulfonate-sensitive21 (MMS21)/high ploidy2 (HPY2)^{16,20}, and protein inhibitors of activated STATs-like1 (PIAL1) and PIAL2²¹. All ligases contain the SP-RING (Siz/PIAS-RING) domain, which functions for SUMO E3 ligase activity. The *siz1-2* *hpy2-1* double mutation causes embryonic lethality²², indicating that these SUMO E3 ligases play important roles in sumoylation in *Arabidopsis* but they have distinct role in development²². Among the >1000 SUMO targets in *Arabidopsis*, few could be assigned to MMS21, whereas numerous targets could be assigned to SIZ1¹⁹, suggesting that MMS21 modifies a small number of proteins and that both SUMO and SIZ1 are crucial regulators of chromatin function and transcription. PIAL1 and PIAL2 function as E4-type SUMO ligases to promote SUMO chain formation and are involved in salt and osmotic stress responses²³. Among these four SUMO E3 ligases, SIZ1 has high similarity to yeast Siz and animal PIAS orthologs²⁴, which contain SAP and SP-RING domains and PINIT (for Pro-Ile-Asn-Ile-Thr) and SXS (Ser-any amino acid-Ser) motifs^{15,25}. However, only plant SIZ proteins contain a PHD (plant homeodomain) finger, which is a C₄HC₃ (four cysteines, one histidine, and three cysteines) zinc-finger-like motif. The PHD finger proteins of ING2 and bromodomain and PHD finger transcription factor (BPTF) recognize trimethylated Lys4 of histone H3 (H3K4me3)^{26,27}. Thus, it is thought that PHDs read the epigenetic code²⁸. Investigation of the PHD finger of rice SIZ1 bound to methylated histone H3 by NMR revealed that OsSIZ1-PHD recognized both dimethylated Arg2 and trimethylated Lys4 of histone H3²⁹. The PHD finger of *Arabidopsis* SIZ1 binds to AtSCE1 and is required for sumoylation of GTE3, a bromodomain protein, together with SP-RING domain, suggesting that PHD and SP-RING contribute to SUMO E3 ligase function³⁰. Although the PHD finger seems to be important for biochemical function, a point mutation in the PHD of *Arabidopsis* SIZ1 complemented several *siz1-2* phenotypes, such as plant growth retardation, thermosensitive seed germination, and hypersensitivity to ABA-induced inhibition of cotyledon

expansion²⁵. Conversely, point-mutated SP-RING was unable to complement the *siz1-2* phenotype²⁵.

To confirm biological importance of the PHD finger in SIZ1, we transformed *ProSIZ1::SIZ1(ΔPHD):GFP* into the *siz1-2* mutant. Although *ProSIZ1::SIZ1:GFP* was able to complement the *siz1* mutation³¹, *ProSIZ1::SIZ1(ΔPHD):GFP* was not, suggesting the biological importance of the PHD finger of SIZ1. In addition, *ProSIZ1::SIZ1(C162S):GFP* was not able to complement it. The biochemical function of PHD is the preferential recognition of histone H3K4me3. Substitution of C162S in the PHD finger prevented recognition of histone H3K4me3, probably preventing complementation of the *siz1-2* mutation. Histone H3K4me3 is enriched with transcriptionally active promoters³². In human cells, recognition of H3K4me3 by ING2-PHD stabilizes the mSin3a–HDAC1 complex to repress active genes in response to DNA damage³³. Because H3K4me3 was highly accumulated in the promoter of *WRKY70* in the *siz1-2* mutant, SIZ1 was suggested to repress active *WRKY70* gene expression via recognition of H3K4me3 by the PHD finger. ATX proteins methylate histone H3K4^{34,35}. The PHD finger also interacts with ATX proteins. It is likely that PHD suppresses the methylation function of ATX proteins. In this article, we demonstrate importance of the PHD finger of SIZ1 on recognition of histone code and transcriptional suppression.

Results

PHD finger is important for SIZ1 function. Plant SUMO E3 ligases, SIZs, contain several motifs and domains, such as SAP (Scaffold attachment factor A/B/acinus/PIAS), PHD, PINIT, SP-RING, SXS, and NLS^{15,25}. Among them, the PHD finger is a unique domain of plant SIZ proteins, whereas SIZ/PIAS proteins in yeast and animals contain no PHD finger. In vitro analysis revealed that the PHD and SP-RING domains of *Arabidopsis* AtSIZ1 are required for binding to the AtSCE1, the SUMO E2-conjugating enzyme, and for sumoylation³⁰. Thus, the PHD finger is assumed to be important for function of AtSIZ1. However, substitution of C134 to tyrosine in the PHD of AtSIZ1 was able to complement phenotypes of the *siz1-2* mutant, such as dwarf-like, thermosensitivity of seed germination, and ABA hypersensitivity²⁵. Expression of *AtSIZ1(C134Y)* in *siz1-2* resulted in abnormal hypocotyl elongation in response to sugar and light, whereas the *siz1-2* mutant did not exhibit such a phenotype²⁵.

To confirm whether the PHD finger is important for SIZ1 function, *ProSIZ1::SIZ1(ΔPHD):GFP* was expressed in the *siz1-2* mutant to complement the dwarf-like phenotype. Expression of *ProSIZ1::SIZ1(ΔPHD):GFP* was unable to complement the dwarf-like phenotype of the *siz1-2* mutant, whereas *ProSIZ1::SIZ1:GFP* was (Fig. 1a). The expression of *SIZ1(ΔPHD):GFP* was confirmed by RT-PCR (Fig. 1b). The results suggest that PHD is important for complementing the dwarf-like phenotype of the *siz1-2* mutant. Then, a substitution was introduced in *ProSIZ1::SIZ1:GFP* and transformed into the *siz1-2* mutant. Because the PHD finger is a C₄HC₃ zinc-finger domain and cysteines and histidine are required for binding to zinc³⁶, *ProSIZ1::SIZ1(C117S):GFP* or *ProSIZ1::SIZ1(C162S):GFP* was expressed in the *siz1-2* mutant. Expression of *SIZ1(C117S)*, as well as *SIZ1(C134Y)*, was able to complement the dwarf-like phenotype²⁵, but *SIZ1(C162S)* was not (Fig. 1a). Expression of *SIZ1* variants was confirmed by RT-PCR (Fig. 1b). These results indicate that C162 in PHD is important for complementation of the *siz1-2* mutation. The amino-acid sequence of the PHD finger in SIZ1 demonstrated that C162 is in an α-helix, whereas C117 and C134 are not (Fig. 1c). It is probable that substitution of C162 to serine severely affects SIZ1 function.

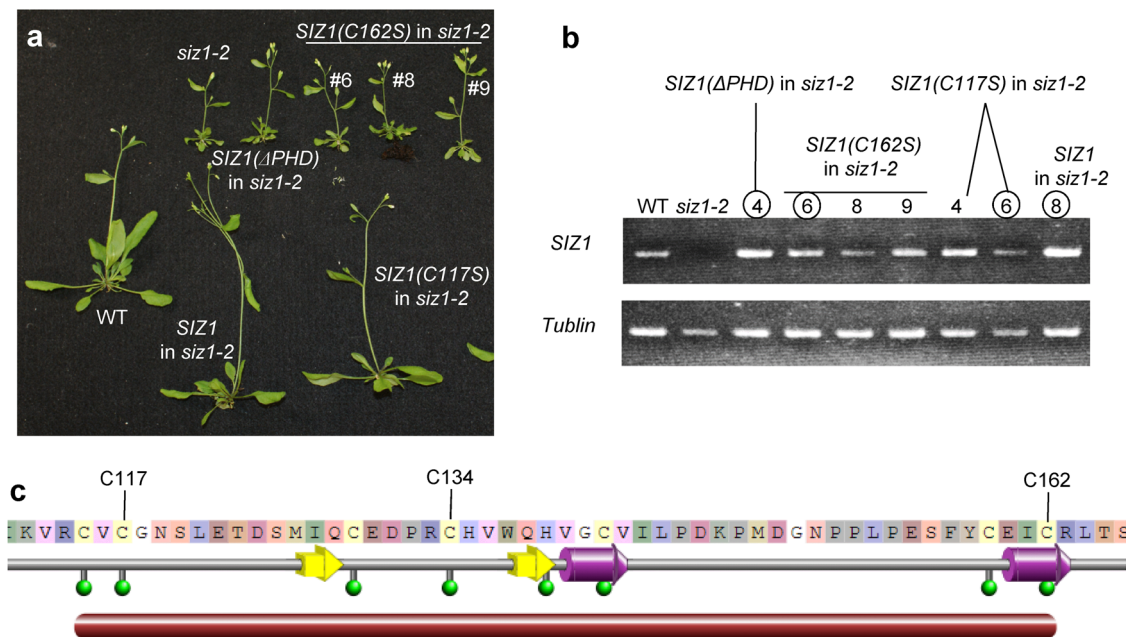


Fig. 1 Mutation in the plant homeodomain (PHD) finger of SIZ1 was unable to complement the dwarf-like phenotype of the *siz1-2* mutant. **a** *ProSIZ1::SIZ1::GFP* or its variants were transformed into the *siz1-2* mutant. Six-week-old *siz1-2* mutant exhibited a dwarf-like phenotype, as previously described³⁹. Introduction of *ProSIZ1::SIZ1::GFP* or *ProSIZ1::SIZ1(C117S)::GFP* complemented the dwarf-like phenotype of *siz1-2*; however, introduction of *ProSIZ1::SIZ1(C162S)::GFP* or *ProSIZ1::SIZ1(ΔPHD)::GFP* was unable to complement the dwarf-like phenotype of *siz1-2*. **b** Expression of *SIZ1* in each plant. *SIZ1* was not detected in the *siz1-2* mutant. Conversely, *SIZ1* transcripts were detected in other plants. **c** Amino-acid sequence and structural information of the PHD finger in SIZ1. Green circles indicate zinc-binding residues. Purple and yellow arrows indicate α -helices and β -sheets, respectively. The illustration was downloaded from Protein Data Bank Japan (PDBj, https://pdj.org/mine/structural_details/1wew).

Next, we examined whether other phenotypes of the *siz1-2* mutant were complemented by expression of *SIZ1* variants. The *siz1-2* mutant exhibited ABA hypersensitivity for primary root growth, compared with wild-type seedlings (Fig. 2a and b)³⁷. Expression of *SIZ1::GFP* or *SIZ1(C117S)::GFP* suppressed the ABA hypersensitivity of *siz1-2* seedlings, whereas expression of *SIZ1(ΔPHD)::GFP* or *SIZ1(C162S)::GFP* did not (Fig. 2 and Supplementary Fig. 1). Furthermore, expression of *SIZ1::GFP* or *SIZ1(C117S)::GFP* complemented the cold sensitivity and drought tolerance of *siz1-2* plants, whereas expression of *SIZ1(ΔPHD)::GFP* or *SIZ1(C162S)::GFP* in the *siz1-2* mutant still exhibited cold sensitivity (Fig. 3 and Supplementary Fig. 2) and drought tolerance (Fig. 4 and Supplementary Fig. 3), indicating that the PHD finger is required for SIZ1 function in response to ABA, cold stress, and drought stress.

PHD recognizes trimethylated histone H3K4. To elucidate the function of the SIZ1 PHD finger, its structure was compared with that in human and rice (Fig. 5). The structures of SIZ1 PHD (1wew), human BPTF PHD (2fuu), and rice SIZ1 PHD (2rsd) have been registered in the PDB database. The PHD finger of human BPTF recognizes histone H3K4me3²⁷. Furthermore, the PHD finger of rice SIZ1 interacts with histone H3K4me3²⁹. Because the structure of the PHD finger of SIZ1 is similar to that of BPTF and that of rice SIZ1 (Fig. 5), it is assumed that the PHD finger of SIZ1 recognizes histone H3K4me3.

The GST-PHD protein was incubated with several types of biotinylated histone H3. Histone H3 was pulled down with streptavidin beads and GST-PHD was detected with an anti-GST antibody. Based on the results of the pull-down assay, PHD interacted weakly with histone H3K4me2 and strongly with H3K4me3 (Fig. 6a). No interaction was detected when histone H3K9me1, H3K4me2, H3K9me3, H3K27me1, H3K427me3, or H3K36me1 was used (Fig. 6a, b). Next, GST-PHD(C162S) or

GST-PHD(C117S) was prepared to confirm whether base substitution influenced the binding activity of PHD. GST-PHD(C162S) was not found to interact with histone H3K4me3 (Fig. 6c), suggesting that disrupting binding with histone H3K4me3 by substitution of cysteine to serine affects the function of SIZ1, as *SIZ1(C162S)::GFP* was unable to complement the *siz1-2* mutation. Conversely, GST-PHD(C117S) was able to bind to histone H3K4me3 (Fig. 6c); thus, the *siz1-2* mutation was complemented by *SIZ1(C117S)::GFP*. Because *siz1-2* plants harboring *SIZ1(C117S)::GFP* looked similar to wild-type plants, the binding activity of PHD(C117S) to histone H3 (Fig. 6c) may not affect the phenotype of the *siz1-2* mutant harboring *SIZ1(C117S)::GFP*. And difference of binding activity of PHD or PHD(C117S) to histone H3K4me3 may not be effective for complementation. For negative control, interaction between GST and histone H3 or H3K4me3 was examined (Fig. 6d).

Histone H3K4me3 status in WRKY70. WRKY70 is a transcription factor that positively regulates SA-responsive genes, and its expression is promoted by increased levels of salicylic acid³⁸. The *siz1-2* mutant accumulates salicylic acid and exhibits a dwarf-like phenotype^{7,39}. Thus, histone H3K4me3 status in the WRKY70 gene was investigated by chromatin immunoprecipitation (ChIP) assay. Under normal conditions, histone H3K4me3 did not accumulate in WRKY70 in the wild type (Fig. 7a). Under cold treatment, histone H3K4me3 was detected in the wild type (Fig. 7a). This is because salicylic acid accumulation was promoted by cold stress, as described previously⁴⁰. On the other hand, the histone H3K4me3 was highly detected in the *siz1-2* mutant under both normal and low-temperature conditions (Fig. 7a). The expression level of WRKY70 was investigated. The transcription of WRKY70 was slightly induced by cold stress (Fig. 7b). WRKY70 expression was higher in the *siz1-2* mutant before and after cold treatment and low expression was observed

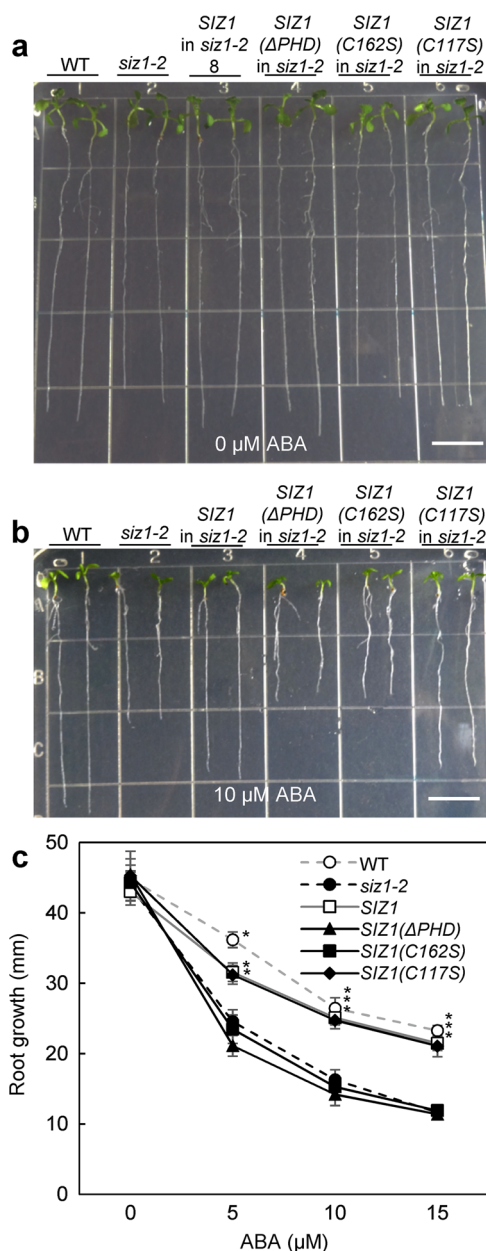


Fig. 2 Mutation in the PHD finger of SIZ1 was unable to complement ABA inhibition of primary root growth in seedlings of the *siz1* mutant. Three-day-old seedlings were transferred onto basal media containing 0 (a) or 10 μ M ABA (b). The bar indicates 1 cm length. c Root growth values expressed as mean \pm standard deviation (SD; $n \geq 15$ biologically independent seedlings). Asterisk indicates a significant difference from the *siz1* plants ($p < 0.05$) as determined by one-way ANOVA followed by the Tukey-Kramer test.

in the *atx1* mutant (Fig. 7b). The expression level of *WRKY70* was correlated with the status of histone H3K4me3. These results suggest that high levels of histone H3K4me3 in the *siz1-2* mutant enhanced expression of the *WRKY70* gene.

Interaction between SIZ1 and ATX1. As shown above, PHD preferentially recognized histone H3K4me3 (Fig. 6), and dysfunction of SIZ1 enhanced H3K4me3 status in the *WRKY70* promoter (Fig. 7). SIZ1 may inhibit methylation of histone H3K4 and prevent transcription initiation via interaction of histone H3K4me3, which is a prominent histone mark associated with

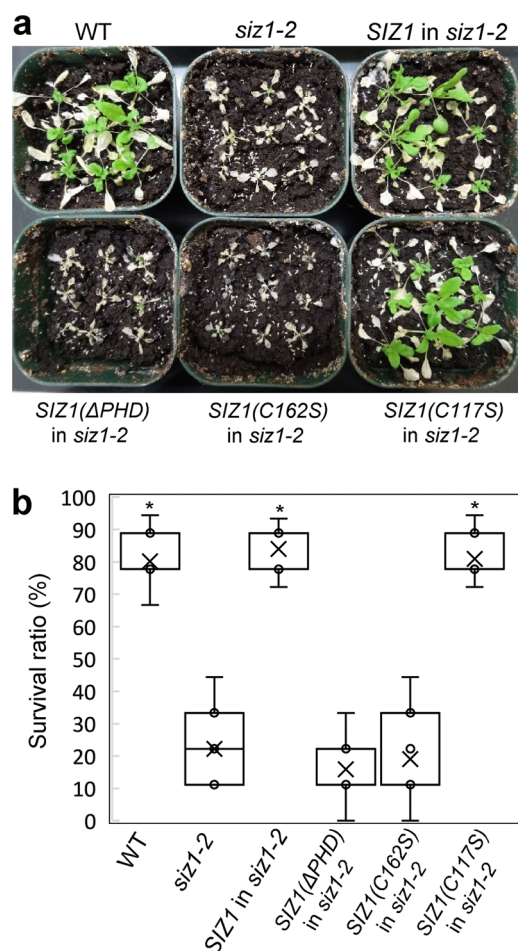


Fig. 3 Cold sensitivity caused by the *siz1-2* mutation was not recovered by SIZ1 with mutation in the PHD finger. a Three-week-old plants were incubated at 4 $^{\circ}$ C for 1 week for cold acclimation. Cold-acclimated plants were exposed for 4 h at -6° C. Following freezing treatment, plants were incubated at 24 $^{\circ}$ C for 1 week. Photographs are representative of WT, *siz1-2*, and *siz1-2* transformed with *SIZ1* variants. b Survival was determined in 27 plants after freezing treatment at -6° C. Data are the mean \pm SD calculated from four or more independent experiments. Asterisks indicate a statistical difference from the *siz1-2* plants ($p < 0.05$) as determined by Student's *t* test.

transcriptionally active genes⁴¹. Among histone lysine methyltransferases, ATX1 mediates H3K4 trimethylation and ATX2 mediates H3K4 dimethylation^{34,35}. Concurrent disruption of the *ATX3*, *ATX4*, and *ATX5* genes significantly reduced H3K4me2 and H3K4me3 levels, suggesting that these are redundant for H3K4 di- and trimethylation⁴². These previous results suggest that ATX1–5 are involved in the transfer of a methyl group to histone H3K4. Thus, we assumed that the PHD finger of SIZ1 interacts with ATX to block activity of histone lysine methyltransferase. ATX1–5 proteins contain catalytic SET domains, which bind S-adenosylmethionine and the substrate lysine⁴³. The SET domains of ATX proteins fused with maltose-binding protein (MBP) were purified, and each MBP-ATXSET was incubated with GST-PHD. After pull-down with GST-PHD, MBP-ATXSET was detected with an anti-MBP antibody. All SET domains were detected by western blot analysis (Fig. 8), indicating that the PHD of SIZ1 was able to interact with the SET domain of each ATX protein. Because GST-PHD(C162S) also detected all SET domains, substitution of C162 in the PHD domain did not affect binding activity to the SET domain of each ATX protein.

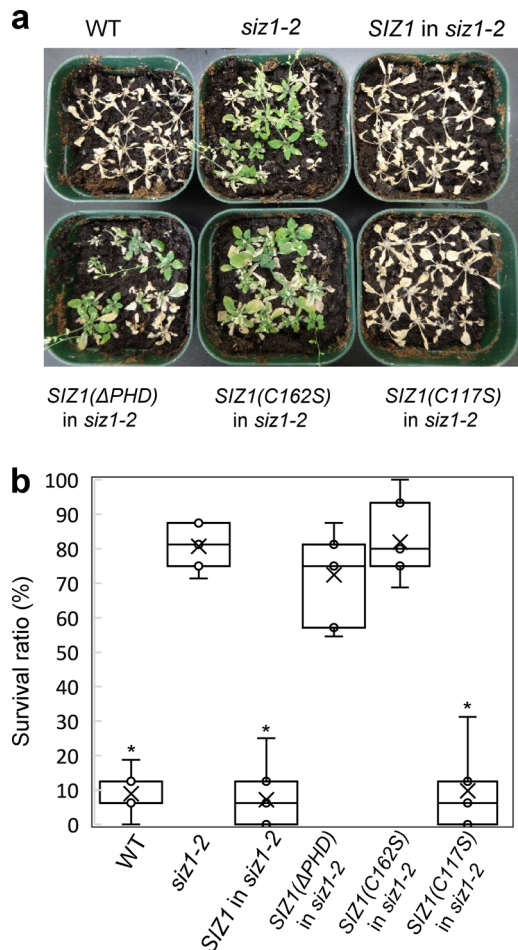


Fig. 4 Drought-tolerant phenotype of the *siz1-2* mutant is not recovered by *SIZ1* with mutation in the PHD finger. **a** Watering was resumed, and plants were incubated for 1 week after the 2-week drought treatment. **b** The survival ratio was determined for 16 plants after drought treatment. Data are mean \pm SD from three independent experiments. Asterisks indicate a statistical difference from the *siz1-2* plants ($p < 0.05$) as determined by Student's *t* test. The data are a representative experiment from three independent experiments.

Probably, PHD has different binding activity to histone H3K4me3 or ATX proteins.

To confirm interaction *in vivo*, full-length coding sequence of *SIZ1* including the PHD finger or ATX1 including the SET domain was inserted into pBYR2HS⁴⁴ fused with the FLAG tag or the RAP tag, respectively. *SIZ1*-FLAG or *SIZ1*(C162S)-FLAG was immunoprecipitated with anti-DYKDDDK antibody. The immunoprecipitant was detected with anti-RAP tag antibody⁴⁵. These results suggest that *SIZ1* interacts with ATX1 *in vivo*.

Discussion

SIZ1 is an important SUMO E3 ligase in plants, and only plant *SIZ* proteins contain a PHD finger⁴⁶. In the present study, we demonstrated that this PHD finger is biologically important, because a mutation or deletion of the PHD finger from *SIZ1* was unable to complement the *siz1-2* mutation (Figs. 1–4). Furthermore, the PHD finger preferentially recognized trimethylated histone H3K4 (Fig. 6a, b). Substitution of C162 with S prevented interaction between the PHD finger and H3K4me3 (Fig. 6c), suggesting that inhibition of PHD (C162S)-binding activity may prevent complementation of the *siz1-2* mutation. The PHD finger also interacted with ATX proteins (Fig. 8), which methylate

histone H3K4, probably resulting in suppressed methylation function of ATX proteins.

Histone H3K4me3 is a landmark of active gene expression⁴⁷. The recognition of H3K4me3 by PHD was first reported in human BPTF and ING2^{26,27,33,48}. PHD recognizes H3K4me3, but it does not affect transcriptional activation or repression, which is dependent on the recruitment of histone acetyl transferase or a histone deacetylase complex. Our results suggest that recognition of H3K4me3 by *Arabidopsis* *SIZ1* induced transcriptional repression of *WRKY70*, because the *siz1-2* mutation promoted its expression (Fig. 7). In mammalian cells, sumoylated histone H4, which is associated with gene repression, in nucleosomes activates LSD1 (lysine-specific demethylase1) by a mechanism dependent on the SUMO-interacting motif in CoREST (co-repressor for element 1 silencing transcription factor)⁴⁹. LSD1 demethylates methylated histone H3K4 to downregulate gene expression. Sumoylated histone H4 enhances development of the LSD1–CoREST complex to repress gene activity. It is plausible that *SIZ1*-bound histone H3K4me3 may recruit demethylase or a co-repressor to repress gene expression in plants.

Although several reports have demonstrated that PHD fingers interact with H3K4me2/3, some bind to other histone marks, such as H3K9me3⁵⁰, H3K36me3⁵¹, H3R2⁵², or unmodified H3K4^{53,54}. PHD fingers are widely conserved in eukaryotic organisms, including plant species. PHD-containing proteins in plants are involved in the regulation of various biological functions, such as pathogen defense responses, developmental processes, and flowering time⁵⁵. These results suggest that PHD has regulatory functions and is involved in the mediation of cross-talk between the epigenetic status of chromatin, and signaling and cellular pathways.

The PHD finger of *Arabidopsis* *SIZ1* interacts with the SUMO E2 enzyme AtSCE1 and the bromodomain global transcription factor group E (GTE)³⁰. The PHD contributes partially to sumoylation of AtSCE1 but is indispensable for sumoylation of GTE³⁰. Similarly, the PHD finger of the human KRAB-associated protein 1 (KAP1) co-repressor binds to the SUMO E2 enzyme Ubc9 and functions as an intramolecular SUMO E3 ligase⁵⁶. The PHD-mediated sumoylation of the adjacent bromodomain is required for gene silencing^{56,57}. Conversely, the PHD finger of rice *SIZ1* was unable to bind to SUMO E2²⁹. These results suggest that the tandem PHD finger-bromodomain, or association between the PHD finger with the bromodomain, is required for transcriptional silencing.

The bromodomain typically recognizes acetylated histones to interpret HAT activity and recognize the histone code⁵⁸. The bromodomain is often found in combination with the PHD finger, as described above. And the bromodomain is also found in combination with other histone-binding domains, including the MBT and WD40 domains⁵⁸. These domains recognize multiple modifications to regulate transcriptional activation or silencing. The NURF chromatin-remodeling complex subunit BPTF harbors a bromodomain and a PHD finger to interact with H4K16ac and H3K4me3, respectively, in the same nucleosome⁵⁹. Conversely, lysine methylation is mediated by SET domain proteins, which are identified in *Drosophila* Su(var)3-9, Ez (Enhancer of Zeste), and Trithorax⁶⁰. Su(var)3-9 methylates histone H3K9, whereas Ez methylates H3K27⁶¹. Trithorax is more likely to mediate methylation of histone H3K4. Based on similarity, five ATX (*Arabidopsis* trithorax) and two ATX-related proteins (ATXR3 and ATXR7) have been proposed as H3K4 methyltransferases⁶². In fact, ATX1, ATX2, and ATXR7 have been shown to be involved in *FLC* activation and histone methylation^{35,63}. To suppress transcription, histone methylation at histone H3K4 should be blocked. The SET domains of ATX proteins interacted with the PHD finger of *SIZ1* (Fig. 8). It is

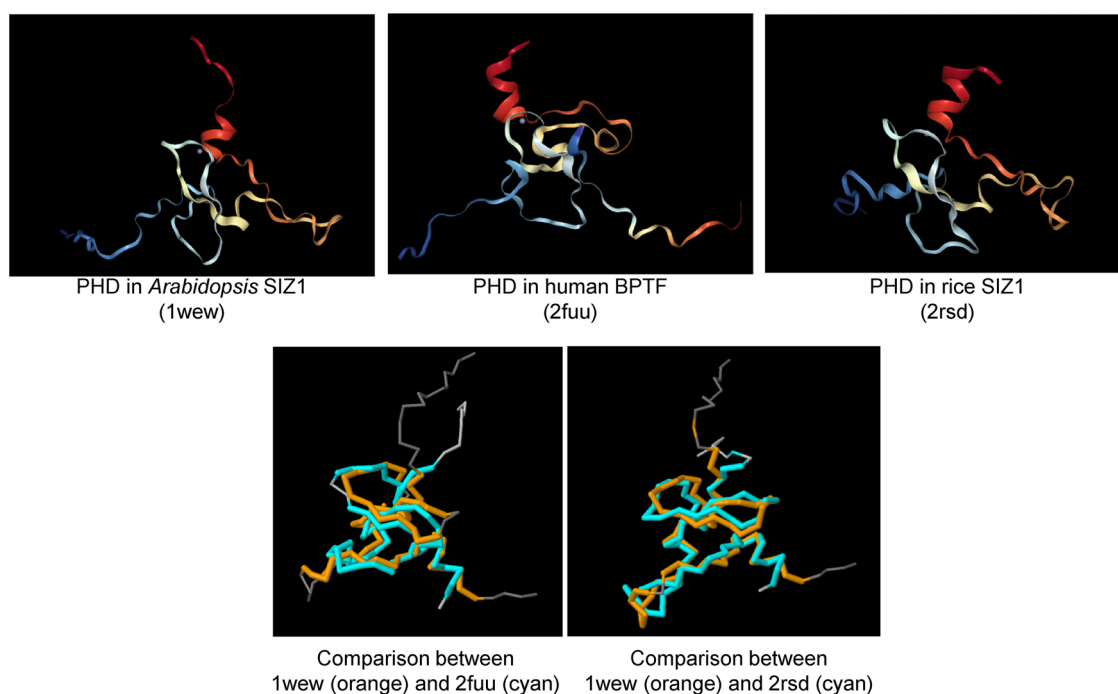


Fig. 5 Comparison of the 3-D structure of the PHD finger in *Arabidopsis* SIZ1 (PDB ID: 1wew) and human BPTF (2fuu) or the PHD finger in rice SIZ1 (PDB ID: 2rsd). The comparison was performed in PDB (<http://www.rcsb.org/pdb/workbench/workbench.do>).

likely that the PHD finger of SIZ1 interacts with ATX proteins to inhibit their access to histone H3K4.

The PHD finger of SIZ1 recognizes histone H3K4me3 and this interaction may suppress transcriptional activation. The PHD finger also binds to ATXs and this interaction may repress methyltransferase activity for further activation of transcription. Because PHD(C162S) was unable to complement the *siz1-2* mutation (Figs. 2–4) and was unable to interact with histone H3K4me3 (Fig. 6) but bound to ATXs (Fig. 8), recognition of histone H3K4me3 is more important for regulation of transcription.

In conclusion, the PHD finger of SIZ1 is important for recognition of the histone code, H3K4me3, to suppress transcription of *WRKY70* and for interaction with ATX proteins, probably to inhibit their binding to histone H3K4.

Methods

Plant materials and physiological analysis. The *Arabidopsis* T-DNA insertion mutants *siz1-2*¹⁵ and *siz1-2* were transformed with pCambia1302-AtSIZ1full::AtSIZ1::GFP and the resulting plants, *siz1-2* with *ProSIZ1::SIZ1::GFP*³¹ were on the Col-0 background.

To produce *siz1-2* with *ProSIZ1::SIZ1(ΔPHD)::GFP*, the 5′- or 3′-regions of SIZ1 were amplified with the primers, SIZ1-2hyF and SIZ1-PHDdeltaR, or SIZ1-PHDdeltaF and SIZ1-2hyR (Supplementary Table 1), respectively. After purification of PCR products, *SIZ1(ΔPHD)* was amplified with the primers, SIZ1-2hyF and SIZ1-2hyR, with the 5′- and 3′-regions of SIZ1 as templates. The PCR product was digested with *Sall* and *PstI* and the resulting product was inserted with *Sall*- and *PstI*-digested pCambia1302-AtSIZ1full::AtSIZ1::GFP. The resulting plasmid, pCambia1302-AtSIZ1full::AtSIZ1(ΔPHD)::GFP, was transformed into *Agrobacterium* and then transgenic Col-0 plants containing *ProSIZ1::SIZ1(ΔPHD)::GFP* were produced. The transgenic Col-0 plant was crossed with the *siz1-2* mutant. In the F2 population, plants harboring both homozygotes of the *siz1-2* mutation and *ProSIZ1::SIZ1(ΔPHD)::GFP* were selected and named *siz1-2* with *ProSIZ1::SIZ1(ΔPHD)::GFP*. The *siz1-2* mutant or wild-type SIZ1 was determined with the primers, LP034008 and Salk_Lba1 or LP034008 and RP0034008 (Supplementary Table 1), respectively. Similarly, pCambia1302-AtSIZ1full::AtSIZ1(C162S)::GFP or pCambia1302-AtSIZ1full::AtSIZ1(C117S)::GFP was produced with the primers, SIZ1-2hyF, AtSIZ1-C162S-R, AtSIZ1-C162S-F, and SIZ1-2hyR, or SIZ1-2hyF, AtSIZ1-C117S-R, AtSIZ1-C117S-F, and SIZ1-2hyR (Supplementary Table 1), respectively. These vectors were transformed and *siz1-2* with *ProSIZ1::SIZ1(C162S)::GFP* or *siz1-2* with *ProSIZ1::SIZ1(C117S)::GFP* were produced. *Arabidopsis*

plants were grown in soil or Petri dishes at 24 °C under a long-day photoperiod (16 h light/8 h dark).

To examine the effect of ABA hypersensitivity on root growth, the seeds were surface-sterilized and sown onto half Murashige and Skoog (MS) medium containing 1% sucrose and 0.8% agar. Three-day-old seedlings were transferred onto media supplemented with 0, 5, 10, or 15 μM ABA (Sigma). Root growth was measured as the difference in root length between the beginning and end of the growth evaluation period²⁴.

To evaluate freezing sensitivity, the plants were grown at 24 °C for 3 weeks in soil and, then incubated at 4 °C for 1 week for acclimation to low temperature. After acclimation, plants were incubated at 0 °C for 1 h, and the temperature was lowered by 2 °C h^{−1} until it reached to −6 °C and was maintained for 4 h in the incubator (IN602, Yamato Scientific Co., Ltd., Tokyo, Japan). Then, plants were incubated at 4 °C overnight and transferred to 24 °C. The survival ratio was determined 10 days after the freezing test was performed, as described previously⁶⁴.

For the drought-tolerance test, water was withheld from 2-week-old plants for 2 weeks. Then, watering was resumed. To quantitatively determine the survival ratio, 16 plants of each genotype were grown in the same pot. After water was withheld followed by re-watering, the survival ratio was calculated as described previously⁴.

These physiological analyses were performed three or more times and representative data were shown in figures.

RNA preparation and RT-PCR. Total RNA was isolated using TRIzol reagent (Thermo Fisher Scientific), according to the manufacturer's protocol. RT-PCR was performed as described previously⁶⁵. The primers LP023805 and RP023805 (Supplementary Table 2) were used to detect *SIZ1* expression. The primers as described in the previous work⁶⁶ were used for detection of *WRKY70* expression. Data are a representative result from three independent experiments.

Pull-down analysis. The PHD region was amplified with the primers pGEX5X-PHD-F and pGEX5X-PHD-R (Supplementary Table 1). The PCR product was inserted into *EcoRI*- and *Sall*-digested pGEX5X-1 (GE healthcare) via the In-Fusion reaction (Takara Bio). The vector was transformed into *Escherichia coli* Rosetta-Gami(DE3)pLysS (Novagen), and GST-PHD protein was purified with Glutathione Sepharose 4 Fast Flow (GE healthcare) according to the manufacturer's protocol. One-microgram of GST-PHD was incubated with 0.5 μg of biotinylated histone H3 variant (Active Motif) in 300 μL of binding buffer (50 mM Tris-HCl, pH 7.8, 300 mM NaCl, 0.1% NP-40, and 1 mM PMSF) overnight. Biotinylated histone H3 variant was pulled down with streptavidin beads. The sample was separated by sodium dodecyl sulfate polyacrylamide gel electrophoresis (SDS-PAGE), and western blot analysis was performed with anti-GST antibody. For input, 10 ng of GST-PHD was loaded. For loading control, 0.5% of mixture before pull-down was loaded onto SDS-PAGE and GST-PHD was detected by anti-GST antibody.

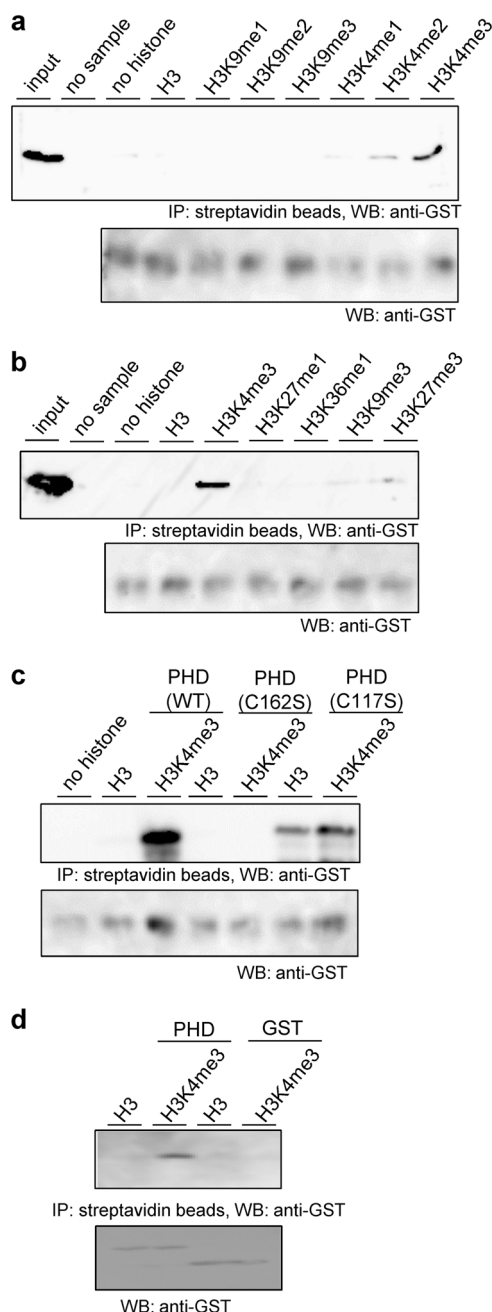


Fig. 6 The PHD finger of SIZ1 recognizes trimethylated histone H3K4me3. The PHD finger was inserted into pGEX5X-1 to produce a GST-PHD fusion protein. GST-PHD fusion proteins were incubated with histone H3 or methylated histone H3 fused with biotin. Pull-down of biotin-histone H3 was performed with streptavidin beads. Then, the proteins were detected by immunoblot analysis with anti-GST. **a** Histone H3 or methylated histone H3K4 or H3K9 were used for pull-down experiments. **b** Pull-down analysis was performed with several types of methylated histone H3. **c** The interaction between GST-PHD variants and histone H3K4me3 was investigated. GST-PHD, GST-PHD(C162S), and GST-PHD (C117S) were prepared and pull-down experiments were performed. **d** For negative control, pull-down assay between GST and histone H3 or H3K4me3 was performed. The bottom panel of each figure is a loading control. Unprocessed blots were provided in Supplementary Fig. 4.

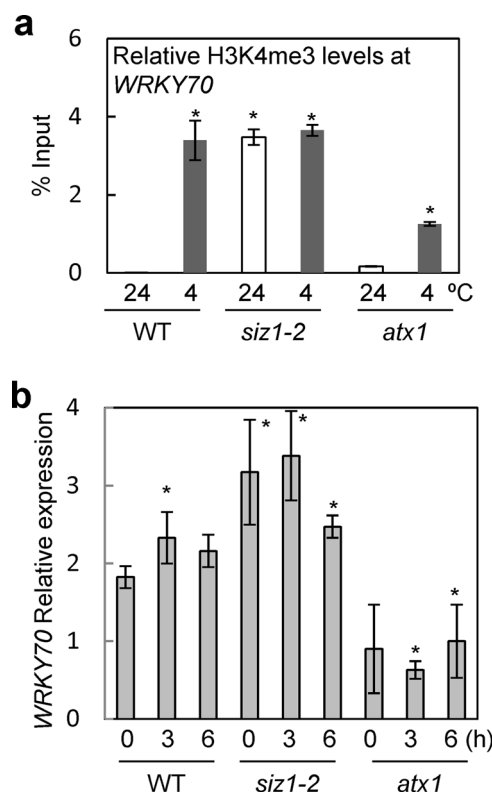


Fig. 7 H3K4me3 levels and transcription of *WRKY70* in the *siz1-2* mutant.

a Levels of histone H3K4me3 at the *WRKY70* gene in wild type and the *siz1-2* mutant. Wild type, the *siz1-2* mutant, and the *atx1* mutant were grown for 3 weeks at 24 °C. The plants were then subjected to cold treatment at 4 °C for 3 h. Then, a ChIP assay was performed. The *atx1* mutant was used as a control to demonstrate that that levels of histone H3K4me3 were low compared with wild type, as described previously⁶⁹. **b** *WRKY70* expression was detected in wild type, the *siz1-2* mutant, and the *atx1* mutant with or without cold treatment. Each experiment was repeated three times and representative data are shown. Each bar represents the standard error of the mean (\pm SE, $n = 3$). Asterisks indicate a statistical difference from the wild type without cold treatment ($p < 0.05$) as determined by Student's *t* test.

The SET domains of ATX proteins were amplified with the primers, ATX(1 or 2)-SET-F-SalI and ATX(1 or 2)-SalI-R (Supplementary Table 1), respectively. The *SalI*-digested PCR products were inserted into the *SalI*-digested pMAL-c2X (New England Biolabs) to produce pMAL-ATX1SET and pMAL-ATX2SET. The SET domains of ATX3–5 were amplified with the primers, ATX(3–5)-F-BamHI and ATX(3–5)-BamHI-R (Supplementary Table 1), respectively. The PCR products and pMAL-c2X were digested with *Bam*HI and ligated. The resulting vectors were named pMAL-ATX(3–5)SET. The vectors were transformed into *E. coli* Rosetta-Gami(DE3)pLysS (Novagen), and MBP-ATXSET protein was purified with amylose resin (New England Biolabs) according to the manufacturer's protocol. One-microgram of GST-PHD and 1 μ g of MAL-ATXSET were incubated in 300 μ L of peptide-binding buffer (50 mM Tris-HCl, pH 7.5, 150 mM NaCl, 0.1% NP-40) overnight. GST-PHD was pulled down with glutathione Sepharose beads. The sample was separated with SDS-PAGE and western blot analysis was performed with an anti-MBP monoclonal antibody (New England Biolabs).

For all immunoblot analysis, the primary antibody was used with 20,000 dilution and the secondary antibody was used with 10,000 dilution.

Co-immunoprecipitation assay. The FLAG tag or the RAP tag was introduced into the high-level transient expression 'Tsukuba system'^{44,67}. The PCR products containing His-tag (HHHHHH), and FLAG tag (DYKDDDDK) were produced with the primers pBYR2HS-Flag-F, FLAG-His, and pBYR2HS-FlagHis-R (Supplementary Table 1). The PCR products containing His-tag (HHHHHH), RAP tag (DMVNPGLIEDRIE)⁴⁵, and the recognition site for HRV 3 C protease (LEVLFGQP), were produced with the primers pBYR2HS-HRV3C-F, HRV3C-RAP-His, and pBYR2HS-stopHis-R (Supplementary Table 1). These PCR products were introduced into the *SalI*-digested pBYR2HS with an In-Fusion HD Cloning

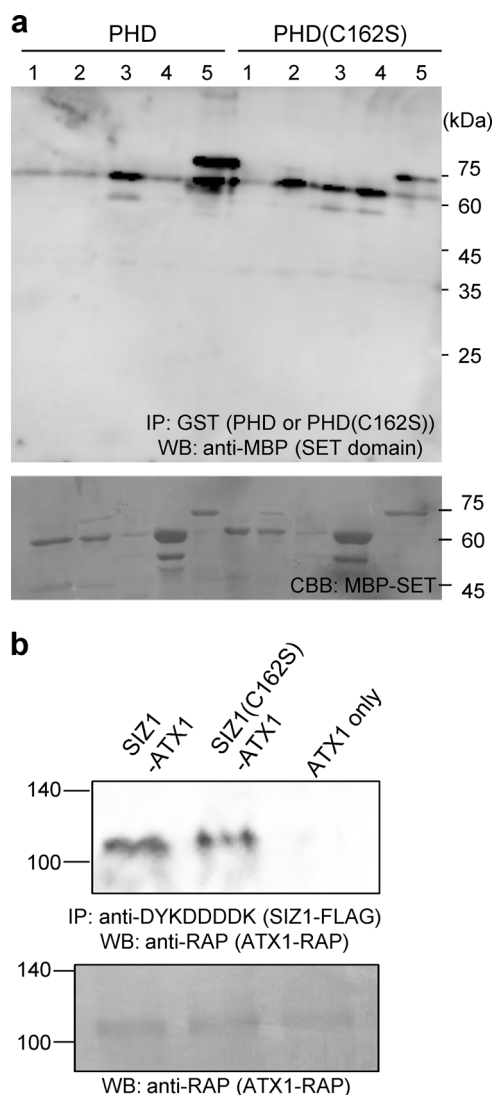


Fig. 8 The PHD finger of SIZ1 interacts with the SET domain of ATX1 proteins. **a** GST-PHD or GST-PHD(C162S) and MBP-ATXSET were incubated and pull-down of GST-PHD or GST-PHD(C162S) was performed with glutathione Sepharose beads. Then, MBP-ATXSET proteins were detected by immunoblot analysis with an anti-MBP monoclonal antibody. Before immunoprecipitation, 5% of protein mixture was loaded onto SDS-PAGE and the gel was stained with Coomassie Brilliant Blue to detect MBP-SET domain of each ATX protein. **b** Interaction between SIZ1 or SIZ1(C162S) and ATX1 in vivo. Entire coding sequence of SIZ1 and ATX1, which are fused with FLAG and RAP, respectively, was transiently expressed in *N. benthamiana*. The immunoprecipitation was performed with anti-DYKDDDDK antibody magnetic beads and the immunoprecipitant was detected by anti-RAP antibody. Unprocessed blot was provided in Supplementary Fig. 4.

Kit. The resulting constructs were designated as pBYR2HS-CFH or pBYR2HS-CRH, respectively. The coding sequence of SIZ1 or ATX1 was amplified with the primers, pBYR2HS-AtSIZ1-F and pBYR2HS-AtSIZ1-R, or pBYR2HS-ATX1-F and pBYR2HS-ATX1-R (Supplementary Table 1), respectively. The resulting PCR products were introduced into the *Sall*-digested pBYR2HS-CFH or pBYR2HS-CRH. pBYR2HS-SIZ1-FH, pBYR2HS-SIZ1(C162S)-FH, or pBYR2HS-ATX1-RH was transformed into *Agrobacterium tumefaciens* GV3101, then, agroinfiltration was performed to *Nicotiana benthamiana*⁴⁴. Soluble protein solution was prepared with lysis buffer⁶⁵. SIZ1-FH or SIZ1(C162S)-FH was immunoprecipitated with anti-DYKDDDDK tag antibody magnetic beads (Fujifilm Wako Pure Chemical Industries). The immunoprecipitant was separated by SDS-PAGE and immunoblot analysis with an anti-RAP tag antibody (PMab2)⁴⁵.

Chromatin immunoprecipitation (ChIP) assay. To investigate histone H3K4me3 status in the promoter of *WRKY70*, a ChIP assay was performed as described previously, with modification⁶⁸. Three-week-old wild-type *siz1-2*, and *atx1* plants (SALK_149002C) were treated with or without cold (4 °C) for 3 h, and the seedlings were subsequently harvested and cross-linked with buffer A (0.4 M sucrose; 10 mM Tris-HCl, pH 8.0; 1 mM EDTA; 1 mM PMSF; 1% formaldehyde). The cross-linking reaction was stopped with 125 mM glycine. The tissues were ground in liquid nitrogen, resuspended in lysis buffer (50 mM HEPES, pH 7.5; 150 mM NaCl; 1 mM EDTA; 1% Triton X-100; 0.1% deoxycholate; 0.1% SDS; 1 mM PMSF; and 1 × protease inhibitor cocktail [Nacalai Tesque]), and sonicated (Microson XL-2000 sonicator, Qsonica, LLC., USA) to achieve an average fragment size of 0.1–1.0 kb. After sonication, centrifugation was performed, and the supernatants were incubated overnight at 4 °C with anti-histone H3K4me3 monoclonal antibody (Active Motif). Immunoprecipitation was performed using Magna ChIP A Chromatin Immunoprecipitation Kits (Millipore). Quantitative PCR was performed with THUNDERBIRD SYBR Premix (Toyobo) using a real-time PCR Thermal Cycler Dice (Takara Bio). The primers, WRKY70-ChipF and WRKY70-ChipR (Supplementary Table 2), were used for detection. The relative quantities of immunoprecipitated DNA fragments were calculated as the percentage of input chromatin that was immunoprecipitated using the comparative C_T method. Data are a representative experiment from three independent experiments.

Statistics and reproducibility. Statistical analysis was performed using Excel software (Microsoft) or IBM SPSS Statics. *P* values < 0.05 were considered significant.

Reporting summary. Further information on research design is available in the Nature Research Reporting Summary linked to this article.

Data availability

The authors declare that all data supporting the findings of this study are available within the paper and its supplementary information files.

Received: 19 March 2019; Accepted: 19 December 2019;

Published online: 10 January 2020

References

- Hendriks, I. A. & Vertegaal, A. C. A comprehensive compilation of SUMO proteomics. *Nat. Rev. Mol. Cell Biol.* **17**, 581–595 (2016).
- Augustine, R. C. & Vierstra, R. D. SUMOylation: re-wiring the plant nucleus during stress and development. *Curr. Opin. Plant Biol.* **45**, 143–154 (2018).
- Zhang, S. et al. A novel tomato SUMO E3 ligase, SIZ1, confers drought tolerance in transgenic tobacco. *J. Integr. Plant Biol.* **59**, 102–117 (2017).
- Miura, K. et al. *SIZ1* deficiency causes reduced stomatal aperture and enhanced drought tolerance via controlling salicylic acid-induced accumulation of reactive oxygen species in Arabidopsis. *Plant J.* **49**, 79–90 (2013).
- Miura, K., Sato, A., Ohta, M. & Furukawa, J. Increased tolerance to salt stress in the phosphate-accumulating Arabidopsis mutants *siz1* and *pho2*. *Planta* **234**, 1191–1199 (2011).
- Miura, K. et al. SIZ1-mediated sumoylation of ICE1 controls *CBF3/DREB1A* expression and freezing tolerance in Arabidopsis. *Plant Cell* **19**, 1403–1414 (2007).
- Lee, J. et al. Salicylic acid-mediated innate immunity in Arabidopsis is regulated by SIZ1 SUMO E3 ligase. *Plant J.* **49**, 79–90 (2007).
- Catala, R. et al. The Arabidopsis E3 SUMO ligase SIZ1 regulates plant growth and drought responses. *Plant Cell* **19**, 2952–2966 (2007).
- Saleh, A. et al. Posttranslational modifications of the master transcriptional regulator NPR1 enable dynamic but tight control of plant immune responses. *Cell Host Microbe* **18**, 169–182 (2015).
- Zheng, Y., Schumaker, K. S. & Guo, Y. Sumoylation of transcription factor MYB30 by the small ubiquitin-like modifier E3 ligase SIZ1 mediates abscisic acid response in Arabidopsis thaliana. *Proc. Natl Acad. Sci. USA* **109**, 12822–12827 (2012).
- van den Burg, H. A., Kini, R. K., Schuurink, R. C. & Takken, F. L. Arabidopsis small ubiquitin-like modifier paralogs have distinct functions in development and defense. *Plant Cell* **22**, 1998–2016 (2010).
- Miura, K. et al. Sumoylation of ABI5 by the Arabidopsis SUMO E3 ligase SIZ1 negatively regulates abscisic acid signaling. *Proc. Natl. Acad. Sci. USA* **106**, 5418–5423 (2009).
- Colby, T., Matthai, A., Boeckelmann, A. & Stuibler, H. P. SUMO-conjugating and SUMO-deconjugating enzymes from Arabidopsis. *Plant Physiol.* **142**, 318–332 (2006).

14. Saracco, S. A., Miller, M. J., Kurepa, J. & Vierstra, R. D. Genetic analysis of SUMOylation in Arabidopsis: conjugation of SUMO1 and SUMO2 to nuclear proteins is essential. *Plant Physiol.* **145**, 119–134 (2007).
15. Miura, K. et al. The Arabidopsis SUMO E3 ligase SIZ1 controls phosphate deficiency responses. *Proc. Natl. Acad. Sci. USA* **102**, 7760–7765 (2005).
16. Ishida, T. et al. SUMO E3 Ligase HIGH PLOIDY2 regulates endocycle onset and meristem maintenance in Arabidopsis. *Plant Cell* **21**, 2284–2297 (2009).
17. Hay, R. T. Decoding the SUMO signal. *Biochem. Soc. Trans.* **41**, 463–473 (2013).
18. Miller, M. J., Barrett-Wilt, G. A., Hua, Z. & Vierstra, R. D. Proteomic analyses identify a diverse array of nuclear processes affected by small ubiquitin-like modifier conjugation in Arabidopsis. *Proc. Natl. Acad. Sci. USA* **107**, 16512–16517 (2010).
19. Rytz, T. C. et al. SUMOylome profiling reveals a diverse array of nuclear targets modified by the SUMO Ligase SIZ1 during heat stress. *Plant Cell* **30**, 1077–1099 (2018).
20. Huang, L. et al. The Arabidopsis SUMO E3 ligase AtMMS21, a homologue of NSE2/MMS21, regulates cell proliferation in the root. *Plant J.* **60**, 666–678 (2009).
21. Tomanov, K. et al. Arabidopsis PIAL1 and 2 promote SUMO chain formation as E4-type SUMO ligases and are involved in stress responses and sulfur metabolism. *Plant Cell* **26**, 4547–4560 (2014).
22. Ishida, T., Yoshimura, M., Miura, K. & Sugimoto, K. MMS21/HPY2 and SIZ1, two Arabidopsis SUMO E3 ligases, have distinct functions in development. *PLoS ONE* **7**, e46897 (2012).
23. Tomanov, K. et al. Arabidopsis PIAL1 and 2 promote SUMO chain formation as E4-type SUMO ligases and are involved in stress responses and sulfur metabolism. *Plant Cell* **26**, 4547–4560 (2014).
24. Miura, K. & Nozawa, R. Overexpression of SIZ1 enhances tolerance to cold and salt stresses and attenuates response to abscisic acid in *Arabidopsis thaliana*. *Plant. Biotechnol.* **31**, 167–172 (2014).
25. Cheong, M. S. et al. Specific domain structures control abscisic acid-, salicylic acid-, and stress-mediated SIZ1 phenotypes. *Plant Physiol.* **151**, 1930–1942 (2009).
26. Pena, P. V. et al. Molecular mechanism of histone H3K4me3 recognition by plant homeodomain of ING2. *Nature* **442**, 100–103 (2006).
27. Li, H. et al. Molecular basis for site-specific read-out of histone H3K4me3 by the BPTF PHD finger of NURF. *Nature* **442**, 91–95 (2006).
28. Li, Y. & Li, H. Many keys to push: diversifying the ‘readership’ of plant homeodomain fingers. *Acta Biochim. Biophys. Sin.* **44**, 28–39 (2012).
29. Shindo, H. et al. PHD finger of the SUMO ligase Siz/PIAS family in rice reveals specific binding for methylated histone H3 at lysine 4 and arginine 2. *FEBS Lett.* **586**, 1783–1789 (2012).
30. Garcia-Dominguez, M., March-Diaz, R. & Reyes, J. C. The PHD domain of plant PIAS proteins mediates sumoylation of bromodomain GTE proteins. *J. Biol. Chem.* **283**, 21469–21477 (2008).
31. Jin, J. B. et al. The SUMO E3 ligase, AtSIZ1, regulates flowering by controlling a salicylic acid-mediated floral promotion pathway and through affects on FLC chromatin structure. *Plant J.* **53**, 530–540 (2008).
32. Liang, G. et al. Distinct localization of histone H3 acetylation and H3-K4 methylation to the transcription start sites in the human genome. *Proc. Natl. Acad. Sci. USA* **101**, 7357–7362 (2004).
33. Shi, X. et al. ING2 PHD domain links histone H3 lysine 4 methylation to active gene repression. *Nature* **442**, 96 (2006).
34. Saleh, A. et al. The highly similar Arabidopsis homologs of trithorax ATX1 and ATX2 encode proteins with divergent biochemical functions. *Plant Cell* **20**, 568–579 (2008).
35. Pien, S. et al. ARABIDOPSIS TRITHORAX1 dynamically regulates FLOWERING LOCUS C activation via histone 3 lysine 4 trimethylation. *Plant Cell* **20**, 580–588 (2008).
36. Pascual, J., Martinez-Yamout, M., Dyson, H. J. & Wright, P. E. Structure of the PHD zinc finger from human Williams-Beuren syndrome transcription factor. *J. Mol. Biol.* **304**, 723–729 (2000).
37. Miura, K. & Hasegawa, P. M. Sumoylation and abscisic acid signaling. *Plant Signal Behav.* **4**, 1176–1178 (2009).
38. Li, J., Brader, G. & Palva, E. T. The WRKY70 transcription factor: a node of convergence for jasmonate-mediated and salicylate-mediated signals in plant defense. *Plant Cell* **16**, 319–331 (2004).
39. Miura, K., Lee, J., Miura, T. & Hasegawa, P. M. SIZ1 controls cell growth and plant development in Arabidopsis through salicylic acid. *Plant Cell Physiol.* **51**, 103–113 (2010).
40. Scott, I. M., Clarke, S. M., Wood, J. E. & Mur, L. A. Salicylate accumulation inhibits growth at chilling temperature in Arabidopsis. *Plant Physiol.* **135**, 1040–1049 (2004).
41. Ruthenburg, A. J., Allis, C. D. & Wysocka, J. Methylation of lysine 4 on histone H3: intricacy of writing and reading a single epigenetic mark. *Mol. Cell* **25**, 15–30 (2007).
42. Chen, L. Q. et al. ATX3, ATX4, and ATX5 encode putative H3K4 methyltransferases and are critical for plant development. *Plant Physiol.* **174**, 1795–1806 (2017).
43. Triebel, R. C., Beach, B. M., Dirk, L. M., Houtz, R. L. & Hurley, J. H. Structure and catalytic mechanism of a SET domain protein methyltransferase. *Cell* **111**, 91–103 (2002).
44. Yamamoto, T. et al. Improvement of the transient expression system for production of recombinant proteins in plants. *Sci. Rep.* **8**, 4755 (2018).
45. Fujii, Y. et al. Development of RAP tag, a novel tagging system for protein detection and purification. *Monoclon. Antib. Immunodiagn. Immunother.* **36**, 68–71 (2017).
46. Miura, K. & Hasegawa, P. M. Sumoylation and other ubiquitin-like post-translational modifications in plants. *Trends Cell Biol.* **20**, 223–232 (2010).
47. Greer, E. L. & Shi, Y. Histone methylation: a dynamic mark in health, disease and inheritance. *Nat. Rev. Genet.* **13**, 343–357 (2012).
48. Wysocka, J. et al. PHD finger of NURF couples histone H3 lysine 4 trimethylation with chromatin remodelling. *Nature* **442**, 86–90 (2006).
49. Dhall, A., Weller, C. E., Chu, A., Shelton, P. M. M. & Chatterjee, C. Chemically sumoylated histone H4 stimulates intranucleosomal demethylation by the LSD1-CoREST complex. *ACS Chem. Biol.* **12**, 2275–2280 (2017).
50. Arita, K. et al. Recognition of modification status on a histone H3 tail by linked histone reader modules of the epigenetic regulator UHRF1. *Proc. Natl. Acad. Sci. USA* **109**, 12950–12955 (2012).
51. Shi, X. et al. Proteome-wide analysis in *Saccharomyces cerevisiae* identifies several PHD fingers as novel direct and selective binding modules of histone H3 methylated at either lysine 4 or lysine 36. *J. Biol. Chem.* **282**, 2450–2455 (2007).
52. Chignola, F. et al. The solution structure of the first PHD finger of autoimmune regulator in complex with non-modified histone H3 tail reveals the antagonistic role of H3R2 methylation. *Nucleic Acids Res.* **37**, 2951–2961 (2009).
53. Ooi, S. K. et al. DNMT3L connects unmethylated lysine 4 of histone H3 to *de novo* methylation of DNA. *Nature* **448**, 714–717 (2007).
54. Tsai, W. W. et al. TRIM24 links a non-canonical histone signature to breast cancer. *Nature* **468**, 927–932 (2010).
55. Mouriz, A., López-González, L., Jarillo, J. A. & Piñeiro, M. PHDs govern plant development. *Plant Signal Behav.* **10**, e993253–e993253 (2015).
56. Ivanov, A. V. et al. PHD domain-mediated E3 ligase activity directs intramolecular sumoylation of an adjacent bromodomain required for gene silencing. *Mol. Cell* **28**, 823–837 (2007).
57. Zeng, L. et al. Structural insights into human KAP1 PHD finger-bromodomain and its role in gene silencing. *Nat. Struct. Mol. Biol.* **15**, 626–633 (2008).
58. Josling, G. A., Selvarajah, S. A., Petter, M. & Duffy, M. F. The role of bromodomain proteins in regulating gene expression. *Genes* **3**, 320–343 (2012).
59. Ruthenburg, A. J. et al. Recognition of a mononucleosomal histone modification pattern by BPTF via multivalent interactions. *Cell* **145**, 692–706 (2011).
60. Bottomley, M. J. Structures of protein domains that create or recognize histone modifications. *EMBO Rep.* **5**, 464–469 (2004).
61. Rea, S. et al. Regulation of chromatin structure by site-specific histone H3 methyltransferases. *Nature* **406**, 593–599 (2000).
62. Ng, D. W. K. et al. Plant SET domain-containing proteins: structure, function and regulation. *Biochim. Biophys. Acta* **1769**, 316–329 (2007).
63. Tamada, Y., Yun, J. Y., Woo, S. C. & Amasino, R. M. Arabidopsis trithorax-related7 is required for methylation of lysine 4 of histone H3 and for transcriptional activation of flowering locus C. *Plant Cell* **21**, 3257–3269 (2009).
64. Mori, K. et al. Ca²⁺-permeable mechanosensitive channels MCA1 and MCA2 mediate cold-induced cytosolic Ca²⁺ increase and cold tolerance in Arabidopsis. *Sci. Rep.* **8**, 550 (2018).
65. Miura, K. et al. *SlICE1* encoding a MYC-type transcription factor controls cold tolerance in tomato, *Solanum lycopersicum*. *Plant Biotechnol.* **29**, 253–260 (2012).
66. Chen, J. et al. Arabidopsis WRKY46, WRKY54, and WRKY70 transcription factors are involved in brassinosteroid-regulated plant growth and drought responses. *Plant Cell* **29**, 1425–1439 (2017).
67. Suzuki, T., Tsuda, M., Ezura, H., Day, B. & Miura, K. Agroinfiltration-based efficient transient protein expression in leguminous plants. *Plant Biotechnol.* **36**, 119–123 (2019).
68. Ohta, M. et al. MYC-type transcription factors, MYC67 and MYC70, interact with ICE1 and negatively regulate cold tolerance in Arabidopsis. *Sci. Rep.* **8**, 11622 (2018).
69. Ding, Y. et al. ATX1-generated H3K4me3 is required for efficient elongation of transcription, not initiation, at ATX1-regulated genes. *PLoS Genet.* **8**, e1003111 (2012).

Acknowledgements

We thank Ms. Kazuko Ito, Ms. Rieko Nozawa, and Ms. Yuri Nemoto at Tsukuba-Plant Innovation Research Center (T-PIRC), University of Tsukuba for technical support. This work was supported by JSPS Grant-in-Aid for Scientific Research on Innovative Areas (JP16H01458 and JP19H04637) and by a Cooperative Research Grant from the Plant Transgenic Design Initiative, Gene Research Center, T-PIRC, University of Tsukuba.

Author contributions

K.M. designed the study. N.R. and K.M. performed most of experiments. T.S. and K.M. contributed reagents and materials and analyzed data. K.M. wrote the manuscript.

Competing interests

The authors declare no competing interests.

Additional information

Supplementary information is available for this paper at <https://doi.org/10.1038/s42003-019-0746-2>.

Correspondence and requests for materials should be addressed to K.M.

Reprints and permission information is available at <http://www.nature.com/reprints>

Publisher's note Springer Nature remains neutral with regard to jurisdictional claims in published maps and institutional affiliations.



Open Access This article is licensed under a Creative Commons Attribution 4.0 International License, which permits use, sharing, adaptation, distribution and reproduction in any medium or format, as long as you give appropriate credit to the original author(s) and the source, provide a link to the Creative Commons license, and indicate if changes were made. The images or other third party material in this article are included in the article's Creative Commons license, unless indicated otherwise in a credit line to the material. If material is not included in the article's Creative Commons license and your intended use is not permitted by statutory regulation or exceeds the permitted use, you will need to obtain permission directly from the copyright holder. To view a copy of this license, visit <http://creativecommons.org/licenses/by/4.0/>.

© The Author(s) 2020